

Carbon Nitride Nanowire Crystals Derived from Pyridine

Xiang Li,^{†,‡} Tao Wang,^{‡,§} Pu Duan,^{||} Maria Baldini,[⊥] Haw-Tyng Huang,^{‡,#} Bo Chen,[¶] Stephen J. Juhl,^{†,‡} Daniel Koeplinger,^{†,‡} Vincent H. Crespi,^{†,‡,§,#} Klaus Schmidt-Rohr,^{||} Roald Hoffmann,[¶] Nasim Alem,^{‡,#} Malcolm Guthrie,[⊗] Xin Zhang,[†] and John V. Badding^{*,†,‡,§,#}

[†]Department of Chemistry, Pennsylvania State University, University Park, Pennsylvania 16802, United States

[‡]Materials Research Institute, Pennsylvania State University, University Park, Pennsylvania 16802, United States

[§]Department of Physics, Pennsylvania State University, University Park, Pennsylvania 16802, United States

^{||}Department of Chemistry, Brandeis University, Waltham, Massachusetts 02453, United States

[⊥]Geophysical Laboratory, Carnegie Institution of Washington, Washington, D.C. 20015, United States

[#]Department of Materials Science and Engineering, Pennsylvania State University, University Park, Pennsylvania 16802, United States

[¶]Department of Chemistry and Chemical Biology, Cornell University, Baker Laboratory, Ithaca, New York 14853-1301, United States

[⊗]European Spallation Source, ESS ERIC, SE-22100 Lund, Sweden

Supporting Information

ABSTRACT: Carbon nanowires are a new one-dimensional sp^3 carbon nanomaterial. They assemble into hexagonal crystals in a room temperature, nontopochemical solid-state reaction induced by slow compression of benzene to 23 GPa. Here we show that pyridine also reacts under compression to form a well-ordered sp^3 product: C_3NH_5 carbon nitride nanowires. Solid pyridine has a different crystal structure from solid benzene, so the nontopochemical formation of low-dimensional crystalline solids by slow compression of small aromatics may be a general phenomenon that enables chemical design of properties. The nitrogen in the carbon nitride nanowires may improve processability, alters photoluminescence, and is predicted to reduce the bandgap.

Relative to the vast corpus of organic molecules, we have few examples of extended carbon networks: diamond, graphite, graphene, and carbon nanotubes. Nevertheless, they have attracted much interest due to their superlative thermal, electronic, and mechanical properties and symmetric geometries.^{1,2} More than 500 new carbon networks have been predicted, but this diversity remains largely unrealized.³ Recently, we showed that polycrystalline benzene transforms under pressure into sp^3 -bonded and one-dimensional^{4,5} single-crystalline packings of carbon nanowires.⁶ Fully saturated degree-6 nanowires^{7,8} could exhibit a unique combination of strength, flexibility, and resilience,^{9,10} whereas partially saturated degree-4 threads may act as novel organic conductors.^{4,6} Moreover, the transformation to nanowire crystal cannot be topochemical¹¹ because it involves large changes in volume and symmetry as multiple short, strong carbon–carbon bonds form between each benzene pair.⁶ Such nontopochemical reactions usually disrupt single-crystalline order and often yield amorphous solid products, but the benzene nanowire reaction instead creates single-crystalline order. The requirement for commensuration between reactant

and product structures for topochemical reactions¹¹ severely constrains the number of suitable monomers; freedom from this requirement could allow for chemical design through solid-state organic synthesis of crystalline extended networks from new types of monomers.

Here we show that slow compression and decompression of polycrystalline pyridine allows for the formation of single-crystal packings of carbon nitride nanowires (Figure 1a,b) with empirical formula C_3NH_5 . Chemical substitution of heteroatoms such as nitrogen into extended carbon networks is generally difficult because nitrogen substituting carbon is not isoelectronic; carbon nitride nanowires, in contrast, are isoelectronic to carbon nanowires. Carbon nitrides are often thought of as compounds that have more N than C (e.g., C_3N_4) to distinguish them from nitrogen-doped carbons.¹² Nonetheless, any solid state compound such as the sp^3 nanowires described here in which nitrogen is intrinsic to the unit cell can be considered a carbon nitride.

The isomeric possibilities and nomenclature for substituted nanowires with chemical formula $((CH)_sX)_n$ (X = heteroatom or -CR substituent) have been explored systematically.¹³ For the isomers of carbon nitride nanowires with chemical formula $((CH)_sN)_n$, we adopt the naming convention of the enumerated carbon nanowires⁵ followed by an integer string that indicates the positions of nitrogen atoms in every six-membered progenitor (i.e., molecular) ring. For example, isomer tube (3,0)_123456 can be generated from the tube (3,0) carbon nanowire where the C–H pairs on positions 1, 2, 3, 4, 5, and 6 of six successive rings in the stack are substituted with N atoms, as shown in Figure 1a,b (see Figure S1 for numbering). Degree-4 unsaturated nanowires have one double bond per pyridine formula (Figure 1c) whereas degree-2 threads have two.⁷

Liquid pyridine was loaded into a double-stage membrane diamond anvil cell.¹⁴ As we slowly compressed the pyridine

Received: December 14, 2017

Published: March 23, 2018

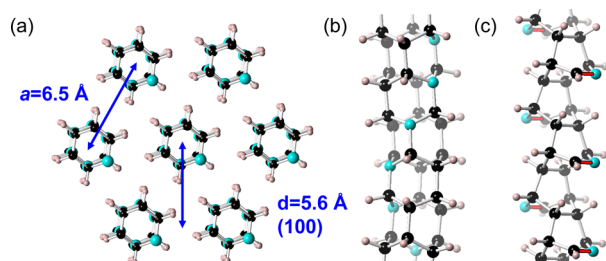


Figure 1. Carbon nitride nanothread structures: (a) view down the hexagonal c axis and (b) view perpendicular to the c -axis of a degree-6 carbon nitride nanothread tube (3,0)₁₂₃₄₅₆. (c) Degree-4 carbon nitride nanothread structure (IV-7) with C–N double bonds in red.

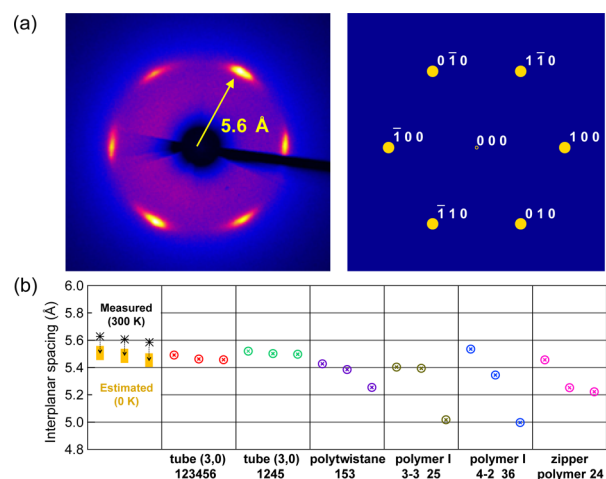


Figure 2. Diffraction experiment and modeling. (a) 6-Fold synchrotron diffraction pattern (left) collected down the hexagonal c axis of the nanothread crystal. Simulated diffraction pattern (right) of carbon nitride tube (3,0)₁₂₃₄₅₆. (b) Experimental and simulated {100} interplanar spacings for the 3 Friedel pairs of carbon nitride nanothread structures. The measured spacings are adjusted for thermal expansion.

over 8–10 h, it first froze to solid pyridine at 1–2 GPa^{15,16} and then reacted at ~18 GPa (Figure S2). A crystalline reaction product has previously been reported, but does not exhibit the diffraction pattern of nanothreads.¹⁷ After holding the sample at 23 GPa for 1 h, the pressure was released to ambient over 8–10 h. The recovered sample is a yellow/orange translucent solid. The diamond cell induces an anisotropic (uniaxial) stress parallel to the force applied by the diamonds.¹⁸

Synchrotron X-ray diffraction patterns collected on the recovered solid (Figure 2a, left) with the beam parallel to the applied uniaxial stress axis are characteristic of a hexagonal single crystal with its c -axis parallel to the X-ray beam, suggesting a role for uniaxial stress in guiding the growth of the crystal.⁶ There is good agreement with the predicted 6-fold single-crystal diffraction pattern of a representative tube (3,0)₁₂₃₄₅₆ carbon nitride nanothread with structural parameters determined by modeling (Figure 2a, right). Additional much weaker $\{hk0\}$ reflections in the [001] zone are evident at smaller interplanar spacings (Figure S3). Again, as for carbon nanothreads, the diffraction patterns for carbon nitride nanothreads are pseudohexagonal,⁶ i.e., with small deviations from perfect hexagonal symmetry. Observation of a pseudohexagonal X-ray diffraction “signature” similar to that observed for carbon nanothreads⁶ provides compelling evidence for the

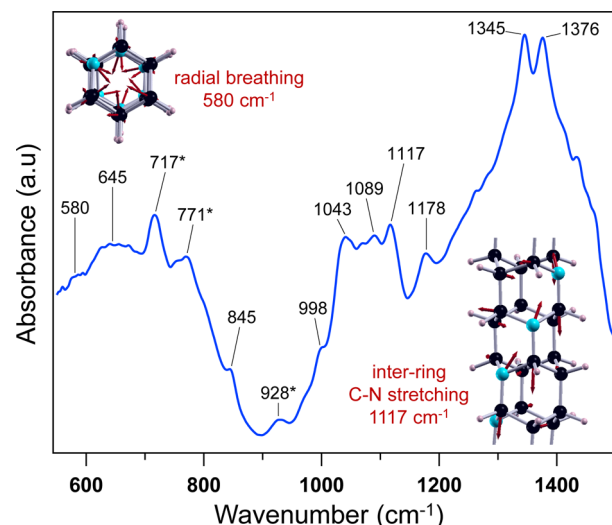


Figure 3. Infrared spectrum. The major radial breathing mode (top left) and the inter-ring C–N stretch mode (bottom right) in tube (3,0)₁₂₃₄₅₆ are shown. Peaks with asterisks may be associated with pyridinic derivatives either as amorphous carbon or as substituted pyridine linking nanothreads. The intensities of these peaks are significantly lower than in the IR spectra of amorphous recovered samples.^{15,16}

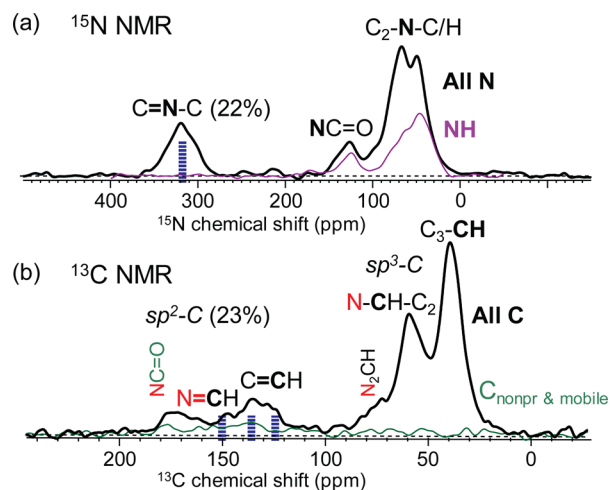


Figure 4. NMR spectra. Solid-state (a) ¹⁵N and (b) ¹³C NMR spectra of nanothreads made from ¹⁵N-enriched pyridine. Peak areas are nearly quantitative. Selective spectra of NH and of nonprotonated C are shown by colored thin lines in panels a and b, respectively. The original signal positions of pyridine are marked by dashed vertical blue lines. The natural-abundance ¹³C spectrum shows the characteristic chemical-shift increases due to N-bonding of nearly half of all C.

synthesis of carbon nitride nanothreads of similar diameter (6.5 Å). Nevertheless, these single-crystal diffraction patterns do not yet constrain which of several possible pyridine nanothread atomic structures¹³ are formed. The ability of uniaxial stress to align nanothreads is remarkable (see also Figure S4). In contrast, other than ref 17, previous investigations of the reaction products from the compression of pyridine reported them to be amorphous,^{15,16} possibly because faster compression/decompression rates led to more highly branched reaction pathways for intermolecular bonding.^{4,6}

The interplanar spacings for the three “pseudohexagonal” Friedel pairs of arcs from experiment can be compared with

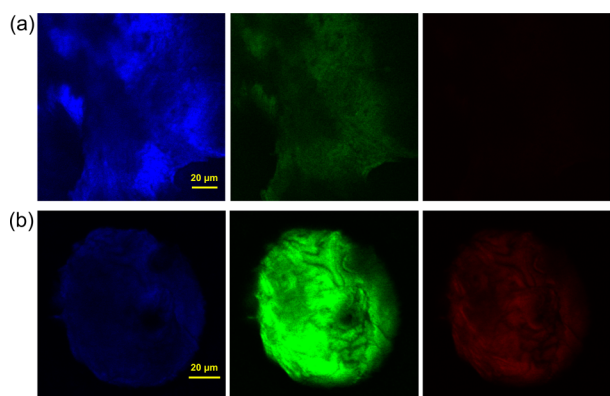


Figure 5. Confocal fluorescence microscopy. Images of blue, green, and red emission from (a) carbon and (b) carbon nitride nanotreads are shown. See SI.

those from simulations (Figure 2b, see also Figure S1 and Supporting Information (SI)) performed at 0 K for six optimized pseudo-hexagonally packed carbon nitride nanotreads, each of which is energetically most stable among their isomeric structures. After shrinking the experimental spacings by 1–3% to account for thermal contraction to 0 K, there is reasonable agreement with the predicted spacings for tube (3,0)₁₂₃₄₅₆. Polytwistane₁₅₃ and zipper polymer₂₄¹³ are also consistent with experiment, but with a slightly denser packing along one dimension (see SI for ideal carbon nitride nanotread structures). Polymer I_{3-3_25} and polymer I_{4-2_36}¹³ seem less likely candidates, with significant differences of spacings when ordered packed, but azimuthal and/or axial packing disorder will narrow the differences among the interplanar spacings.

Amorphous carbon nitride (*a*-C:H:N) films deposited by chemical vapor deposition have broad infrared (IR) absorption spectra.¹⁹ In contrast, carbon nitride nanotreads exhibit more and narrower absorption features (Figure 3) suggestive of greater structural order not only of the thread packing (Figure 2) but also of the atomic structure along the thread axis (see also SI). We calculated the IR absorption spectra of the six candidate structures mentioned above. Two notable characteristic vibrations of a 1D thread or tube are radial breathing and axial elongation-compression modes.¹ The former is Raman (but not IR) active in carbon nanotreads and is observed experimentally at 805 cm⁻¹,⁴ much higher in frequency than corresponding modes for (larger-diameter) sp² carbon nanotubes.¹ Symmetry breaking due to the nitrogen atoms in carbon nitride threads splits this mode and makes it IR active. In all of the simulated spectra, there are one or several absorption peaks from 575 to 650 cm⁻¹ associated with radial breathing. In contrast to the corresponding higher-symmetry pure-carbon threads, mode eigenvectors for the radial breathing modes of carbon nitride threads include nonradial (axial, circumferential) motions, the magnitudes of which depend on the precise nitrogen placements on successive rings.

Considering the complexity of the vibrational modes in this region and the possibility of more than one type of nanotread forming during reaction, these calculated modes are consistent with the broad peaks observed in experiment at 580 and 645 cm⁻¹. Axial elongation and compression in carbon nitride nanotreads include stretching of both C–C and C–N single bonds formed between pyridine rings upon reaction. A peak in the IR spectrum at 1117 cm⁻¹ is identified as inter-ring C–N

stretching because all the calculated spectra show this mode near 1120 cm⁻¹ with moderate-to-strong intensity. Unlike the peak at 1178 cm⁻¹ that is associated with intra-ring C–C and C–N stretching, neither the 1117 cm⁻¹ inter-ring peak nor the radial breathing modes near 600 cm⁻¹ appear in prior samples derived from pyridine at high pressure (Figure S5),¹⁵ i.e., they seem to be diagnostic of a thread-like structure, although the current IR spectra cannot yet uniquely determine which thread structure is formed.¹³ The SI provides detailed discussion of assignments, comparison with other candidate structures, modeling methods and animated vibrations.

We prepared larger (mg) samples in a Paris-Edinburgh press for chemical analysis (Materials and Methods, Figure S4). Only C, N, and O were found in X-ray photoelectron spectroscopy scans (Figure S6). The observed C:N ratio, 5.08:1, is very close to that of pyridine, which contrasts with chemical vapor deposition approaches for sp² systems, which form low nitrogen content ($x = 0.01–0.02$) CN_x nanotubes when using pyridine as a precursor.²⁰ Bulk combustion analysis gave a reasonably close composition, 5.5:1, whereas nuclear magnetic resonance (NMR) analysis gave 4.1 ± 0.9:1 (see SI for details).

¹⁵N and ¹³C solid-state NMR spectra collected on ¹⁵N-enriched carbon nitride nanotreads (Figure 4) reveal nearly identical sp²/sp³ ratios for nitrogen and carbon (22–23% sp², 77–78% sp³), indicating significant conversion from sp²- to sp³-bonding during polymerization and similar outcomes for C and N. About 45% of sp³ carbons have chemical shifts between 50 and 95 ppm, indicating that they are bonded to N. This exceeds the C–N bond fraction of 2/5 = 40% in pyridine and thus indicates C–N bond formation between pyridine rings, which is consistent with the observation of inter-ring C–N stretching in IR. While the ¹⁵N chemical shift of ~310 ppm is similar for pyridine and imine N=CH, the pronounced CH resonances near 170 ppm in the ¹³C spectrum, distinct from pyridine signals at ≤152 ppm, document the presence of imine N=CH as found in degree-4 nanotreads.

Furthermore, the relative ¹³C NMR peak intensities indicate that in degree-4 threads, N=CH is strongly favored over N–CH=CH, which would produce a CH peak near 106 ppm that is not significantly observed in Figure 4b. The estimated fraction of degree-6 carbon nitride nanotreads is ca. 40%, after taking into account the sp³-hybridized carbons associated with degree-4 nanotreads. These two different types of threads still appear to pack into ordered crystals (Figure 2a). Figure 4a and Figures S8 and S9 also show some amides and N–H moieties, which may be due to reaction with O₂ and/or H₂O from air.

Synthesis of nanotreads from benzene^{4,6} and pyridine with distinct progenitor molecular crystal structures²¹ suggests that general principles govern nanotread formation. Under compression, an efficient molecular packing forms stacks of parallel aligned flat molecules. Such stacks provide a natural direction for a polymerization that yields 1D structures, i.e., nanotreads. The small size of the rings impedes π overlap between molecules in adjacent stacks, disfavoring cross-link polymerization to form 2D networks. The uniaxial component of the applied stress defines the thread axis, and the enthalpic driving force for efficient packing under pressure strongly favors a dense near-hexagonal packing of the threads. Low (i.e., room) reaction temperature favors the single lowest-barrier kinetic pathway toward thread formation and requires slow compression and decompression to afford the reaction sufficient time to proceed.

Nanotreads exhibit photoluminescence, likely due to defects or sp^2 carbon functions along their length (Figure 5a,b) or bandgap emission.^{22,23} The blue, green, and red emission properties of carbon nitride nanotreads differ from those of carbon nanotreads (Figure 5 a,b, Figures S10 and S11). The shift to longer emission wavelengths for carbon nitride nanotreads is likely to be associated with the decrease in bandgap predicted for carbon nanotreads²⁴ or nitrogen-related defects. Thus, with further synthesis work nanotreads might be chemically designed for specific biological imaging applications.²³

■ ASSOCIATED CONTENT

Supporting Information

The Supporting Information is available free of charge on the ACS Publications website at DOI: 10.1021/jacs.7b13247.

Degree-6 carbon nitride nanotread structure: Polymer I_3-3_25 (CIF)

Degree-6 carbon nitride nanotread structure: Polymer I_4-2_36 (CIF)

Degree-6 carbon nitride nanotread structure: Polytwistane_153 (CIF)

Degree-6 carbon nitride nanotread structure: Tube (3,0)_1245 (CIF)

Degree-6 carbon nitride nanotread structure: Tube (3,0)_123456 (CIF)

Degree-6 carbon nitride nanotread structure: Zipper polymer_24 (CIF)

Degree-4 carbon nitride nanotread structure: IV-7 (CIF)

Vibrational mode animations (ZIP)

Materials and Methods, Additional Discussion (PDF)

■ AUTHOR INFORMATION

Corresponding Author

*j.badding@chem.psu.edu

ORCID

Bo Chen: 0000-0002-5084-1321

Klaus Schmidt-Rohr: 0000-0002-3188-4828

Ronald Hoffmann: 0000-0001-5369-6046

Xin Zhang: 0000-0001-6686-1645

John V. Badding: 0000-0002-4517-830X

Notes

The authors declare no competing financial interest.

■ ACKNOWLEDGMENTS

We acknowledge the Energy Frontier Research in Extreme Environments (EFREE) Center, an Energy Frontier Research Center, funded by the Department of Energy (DOE) Office of Science (DE-SC0001057). Samples were synthesized at the Spallation Neutrons and Pressure beamline (SNAP) at the Spallation Neutron Source, a DOE Office of Science User Facility operated by Oak Ridge National Laboratory and the High-Pressure Neutron Diffractometer beamline (PLANET) at the Japan Proton Accelerator Research Complex. X-ray diffraction was performed at the High-Pressure Collaborative Access Team (HPCAT) beamlines 16 BM-D and 16 ID-B at the Advanced Photon Source (APS), Argonne National Laboratory. HPCAT is supported by DOE-NNSA (DE-NA0007), with partial instrumentation support from the National Science Foundation. We thank C. Park and H.

Yennawar for assistance with APS and laboratory X-ray diffraction, respectively.

■ REFERENCES

- (1) Dresselhaus, M. S.; Dresselhaus, G.; Eklund, P. *Science of Fullerenes and Carbon Nanotubes: Their properties and Applications*; Elsevier: New York, 1996.
- (2) Rao, C. N. R.; Sood, A. K. *Graphene: synthesis, properties, and phenomena*; Wiley-VCH: Weinheim, Germany, 2013.
- (3) Hoffmann, R.; Kabanov, A. A.; Golov, A. A.; Proserpio, D. M. *Angew. Chem., Int. Ed.* **2016**, *55*, 10962–10976.
- (4) Fitzgibbons, T. C.; Guthrie, M.; Xu, E. S.; Crespi, V. H.; Davidowski, S. K.; Cody, G. D.; Alem, N.; Badding, J. V. *Nat. Mater.* **2015**, *14*, 43–47.
- (5) Xu, E. S.; Lammert, P. E.; Crespi, V. H. *Nano Lett.* **2015**, *15*, 5124–5130.
- (6) Li, X.; Baldini, M.; Wang, T.; Chen, B.; Xu, E.-s.; Vermilyea, B.; Crespi, V. H.; Hoffmann, R.; Molaison, J. J.; Tulk, C. A.; Guthrie, M.; Sinogeikin, S.; Badding, J. V. *J. Am. Chem. Soc.* **2017**, *139*, 16343–16349.
- (7) Chen, B.; Hoffmann, R.; Ashcroft, N. W.; Badding, J.; Xu, E. S.; Crespi, V. H. *J. Am. Chem. Soc.* **2015**, *137*, 14373–14386.
- (8) Olbrich, M.; Mayer, P.; Trauner, D. *J. Org. Chem.* **2015**, *80*, 2042–2055.
- (9) Roman, R. E.; Kwan, K.; Cranford, S. W. *Nano Lett.* **2015**, *15*, 1585–1590.
- (10) Zhan, H.; Zhang, G.; Tan, V. B. C.; Cheng, Y.; Bell, J. M.; Zhang, Y.-W.; Gu, Y. *Nanoscale* **2016**, *8*, 11177–11184.
- (11) Toda, F. *Organic Solid-State Reactions*; Springer: Berlin, 2005.
- (12) Miller, T. S.; Jorge, A. B.; Suter, T. M.; Sella, A.; Cora, F.; McMillan, P. F. *Phys. Chem. Chem. Phys.* **2017**, *19*, 15613–15638.
- (13) Chen, B.; Wang, T.; Crespi, V. H.; Li, X.; Badding, J.; Hoffmann, R. *J. Chem. Theory Comput.* **2018**, *14*, 1131–1140.
- (14) Sinogeikin, S. V.; Smith, J. S.; Rod, E.; Lin, C.; Kenney-Benson, C.; Shen, G. *Rev. Sci. Instrum.* **2015**, *86*, 072209.
- (15) Fanetti, S.; Citroni, M.; Bini, R. *J. Chem. Phys.* **2011**, *134*, 204504.
- (16) Zhuravlev, K. K.; Traikov, K.; Dong, Z.; Xie, S.; Song, Y.; Liu, Z. *Phys. Rev. B: Condens. Matter Mater. Phys.* **2010**, *82*, 064116.
- (17) Yasuzuka, T.; Komatsu, K.; Kagi, H. *Chem. Lett.* **2011**, *40*, 733–735.
- (18) Yao, M. G.; Fan, X. H.; Zhang, W. W.; Bao, Y. J.; Liu, R.; Sundqvist, B.; Liu, B. B. *Appl. Phys. Lett.* **2017**, *111*, 101901.
- (19) Ferrari, A. C.; Rodil, S. E.; Robertson, J. *Phys. Rev. B: Condens. Matter Mater. Phys.* **2003**, *67*, 155306.
- (20) Liu, J.; Czerw, R.; Carroll, D. L. *J. Mater. Res.* **2005**, *20*, 538–543.
- (21) Podsiadlo, M.; Jakobek, K.; Katrusiak, A. *CrystEngComm* **2010**, *12*, 2561–2567.
- (22) Rusli; Robertson, J.; Amaratunga, G. A. J. *J. Appl. Phys.* **1996**, *80*, 2998–3003.
- (23) Hong, G. S.; Diao, S. O.; Antaris, A. L.; Dai, H. J. *Chem. Rev.* **2015**, *115*, 10816–10906.
- (24) Silveira, J. F. R. V.; Muniz, A. R. *Phys. Chem. Chem. Phys.* **2017**, *19*, 7132–7137.